

Solid state synthesis, characterization and biological evaluation of silver doped nanosized metal oxides

G. Tanuja^a, Sangappa K Ganiger^b, Shashidhar^c, R.K. Preeti^d, Somanath Reddy Patil^e and Arunkumar Lagashetty^{f*}

^aDepartment of Nanotechnology, Regional Research Centre, VTU, Belagavi, 580018, Karnataka, India

^bDepartment of Physics, Government Engineering College, Raichur, 584135, Karnataka, India

^cDepartment of Chemistry, SDM College of Engineering and Technology, Dharwad-580002, Karnataka, India

^dDepartment of Zoology, Gulbarga University, Kalaburagi-585103 Karnataka, India

^eDepartment of Zoology, Govt. First grade College, Kalaburagi-585103 Karnataka, India

^fDepartment of Studies in Chemistry, Vijayanagar Sri Krishna devaraya University, Ballari, 583105, Karnataka, India

CHRONICLE

Article history:

Received December 20, 2022

Received in revised form

January 28, 2023

Accepted March 28, 2023

Available online

March 28, 2023

Keywords:

Metal Oxide

XRD

SEM

FTIR

Biological activity

ABSTRACT

Nanomaterials have attracted a great deal of attention from the scientific community due to their unique properties and applications. The small size metal oxides have opened up the door for intensive research to utilize their properties for biomedical applications. Silver nanoparticle (AgNPs) and metal oxide nanomaterials like MgO, ZnO, NiO and its silver doped nanocomposites (Ag-MgO, Ag-ZnO, Ag-NiO) have been prepared using solid state combustion method using polyvinyl alcohol (PVA) as a fuel. The structure of as prepared oxides and its silver doped nanocomposites were characterized using X-ray diffraction (XRD) tool and morphology by Scanning Electron Micrograph (SEM) tool as well as Transmission electron micrograph tool respectively. Presence of the metals in the oxides and its Ag composite was confirmed by the EDX pattern. Bonding nature in the composite is well studied by the Fourier transform infrared (FT-IR) tool. Antibacterial activity studies of the nanocomposites are carried out against various bacteria.

© 2023 by the authors; licensee Growing Science, Canada.

1. Introduction

Nanomaterials and its technologies are enticed and magnetized in recent and upcoming research. Integration of the science and technology at nano dimension attracts the researchers due to the progressive applications¹⁻³. The latest physical properties and advanced technologies both in sample preparation and device fabrication evoke on account of the progress of nanoscience⁴⁻⁵. The man in his quest for knowledge has been conceiving and developing the physical world and its components in bigger than the biggest and smaller than the smallest dimensions of mass, length and time⁶⁻⁷. Sometimes the changes in particle size are to such an extent that completely new transpirations are dig up which helps in flowering of the world⁸⁻⁹. However, the title is about how the biological activity takes place for certain materials when it is reduced into nanoscale dimensions. In this world of elaboration nanotechnology, one of the main primary concerns should be the potential environmental impact of nanoparticles (NPs). A proper way of estimating the nanotoxicity is to monitor the response of the bacteria against these nanoparticles¹⁰⁻¹².

Inorganic nanoparticles (NPs), metal oxides are the most interesting NPs due to their applications and positive impact on pathogenic microorganisms¹³⁻¹⁵. NPs have been studied for many years because of their size-dependent physical and

* Corresponding author.

E-mail address arun.lagashetty@gmail.com (A. Lagashetty)

chemical properties. Among NPs, great attention has been shifted to monoxides¹⁶⁻¹⁸. Nps have attracted great interest due to their special or specific properties and selectivity, especially in pharmaceutical and biological applications¹⁹. In laboratory tests with NPs, different microorganisms have been eliminated within minutes of contact with the NPs²⁰⁻²¹. The application of NPs on bacteria is very important since NPs have a tendency to be in the lowest level and directly enter the food chain of the ecosystem²².

Resistance of bacteria to bactericides and the higher generation antibiotics has increased in the latest years due to the flowering of resistance strains. Recently, it has been demonstrated that highly reactive metal oxide nanoparticles exhibit exoticbiocidal action against Gram-positive and Gram-negative bacteria²³. This is the preparation, characterization, surface modification, and implementation of a very blooming generation of bactericidal materials. The toxicity is calculated on both the exposure and the size of the metal nanoparticles like alumina, copper, gold, magnesium, cobalt, barium, silver, titanium, and zinc. Metal oxide is not only stable but generally it is said to be as safe to human beings²⁴. There are several investigations that have been found and are also being focused on the investigation of their properties of metal oxide nanoparticles. The toxicity of these nanoparticles is tested or can be recognized by two methods firstly, culturing in liquid media containing nanoparticles, and electro spraying the nanoparticles directly onto the bacteria surface. Ferrites are chemical compounds which come across as powder or ceramic bodies with ferrimagnetic properties achieved by iron oxides as their main component, Fe₂O₃ and FeO, which can be partly replaced by other transition metal oxides²⁵.

It is reported in the literature that noble metals like Ag metal show good antimicrobial activity against various bacteria and fungi. The antimicrobial activity results of Ag metal are compared with results of metal oxides showing considerable increase in the activity. To enhance the antimicrobial activity of metal oxides by doping active Ag metal to the prepared metal oxides. Hence, the novelty of this experimentation is to prepare single phase metal oxides by combustion route and enhance its biological activity by Ag metal doping by the same combustion route. The present study reports the synthesis of Ag metal, metal oxides like MgO, NiO and ZnO and Ag doped metal oxides using combustion method through metal carboxylate as precursor. PVA is used as a fuel for the combustion process. Prepared samples are well characterised by various characterisation techniques such as XRD, SEM, IR, EDX etc. Antibacterial activity study of the Ag doped above metal oxides is carried out against various bacteria.

2. Materials and Methods

All chemicals utilized as a part of these trials are of AR grade evaluation. PVA (Polyvinyl alcohol) is utilized as a fuel for strong state ignition response for union of nanosized metal oxide material. Double refined water is utilized as a solvent and acetone is used for the separation of the carbon particles.

2.1 Synthesis of metal oxalates

The magnesium oxalate is prepared by dissolving a known quantity of magnesium chloride and oxalic acid in 100 ml of double distilled water in a separate container with the molar ratio of 1:1 respectively. These solutions are mixed together in a separate container and kept on the magnetic stirrer for 1 hour to complete conversion of magnesium chloride into its oxalate by reacting with oxalic acid. Finally, magnesium oxalate precipitate is washed with distilled water and dried by passing hot air with minimum pressure. Similar procedure is adopted for the preparation of nickel oxalate and zinc oxalate by reacting nickel and zinc salts with oxalic acid¹⁵. The possible synthetic reactions are given in **Table 1**²⁶.

2.2 Synthesis of nanosized silver (Ag) metal

In the typical combustion process, the silver oxalate is burned with the poly (vinyl alcohol) (PVA) as a fuel with the molar ratio of 1:5; the combustion reaction is arrested at the particular temperature for the phase formation. The impurities present in the final product are separated by treatment with acetone and dried.

2.3 Synthesis of MgO, NiO and ZnO nanoparticles

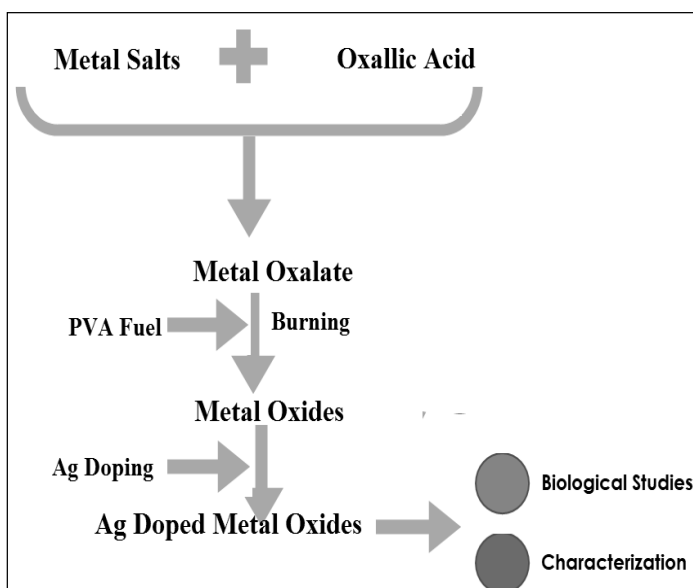
Combustion route is used for the synthesis of magnesium oxide materials using PVA as a fuel for the burning reaction. The prepared magnesium oxalate is mixed with PVA in the weight ratio 1:5 and ground well using pestle and mortar. The mixture was transferred into a crucible and ignited in an electrical oven. The dispersed phase ignited with the evolution of a large volume of gases and these gases completed within a short time. During burning, PVA reacts with the precursor and only a partially decomposed product is obtained. The temperature of the process does not exceed 300 °C at any time. Chemical and physical characterisation of the partially decomposed products did not give any confirmable phases. The possible reason for a partially decomposed product formed may be attributed to the low temperature of the reaction giving rise to the insufficient energy needed for complete conversion. However, the samples are further heated continuously for about 30-40 minutes. The solids burn completely and leave behind magnesium oxide. Similar procedure is used to prepare NiO and ZnO using nickel oxalate and zinc oxalate respectively. The possible reactions involved in the synthetic process are given in **Table 1**.

Table 1. Possible chemical reactions of metal and metal oxides

Sl.No.	Sample	Chemical reactions
	Ag	$\text{Ag}^+ \rightarrow \text{Ag}$
1	MgO	$\text{MgCl}_2 + (\text{COOH})_2 \rightarrow \text{Mg}(\text{C}_2\text{O}_4) + 2\text{HCl}$ $\text{Mg}(\text{C}_2\text{O}_4) + 1/2\text{O}_2 \rightarrow \text{MgO} + 2\text{CO}_2$
2	NiO	$\text{NiCl}_2 + (\text{COOH})_2 \rightarrow \text{Ni}(\text{C}_2\text{O}_4) + 2\text{HCl}$ $\text{Ni}(\text{C}_2\text{O}_4) + 1/2\text{O}_2 \rightarrow \text{NiO} + 2\text{CO}_2$
3	ZnO	$\text{ZnCl}_2 + (\text{COOH})_2 \rightarrow \text{Zn}(\text{C}_2\text{O}_4) + 2\text{HCl}$ $\text{Zn}(\text{C}_2\text{O}_4) + 1/2\text{O}_2 \rightarrow \text{ZnO} + 2\text{CO}_2$

2.4 Synthesis of Ag doped metal oxide nanomaterials

Magnesium oxide nanomaterials are doped with the silver metal nanoparticles (Ag-MgO) using the combustion method. The process starts with burning of magnesium oxide with silver metal nanoparticles and PVA keeping the molar ratio as 2:1:5 respectively. These samples were grinded well in pestle and mortar and transferred to the China crucible. Initially, it burns in an electrical oven for completion of white dense fumes, after this it will start burning with sooty flame followed by reduced non sooty flame for complete reaction. This reaction was arrested at a particular temperature around 500°C for about half an hour to form the phase Ag-MgO nanoparticles. Later it is washed with acetone and concentrated action to remove the carbon particles and other organic impurity. Similar procedure is used for the synthesis of Ag-NiO and Ag-ZnO nanoparticles. The synthetic scheme of Ag doped metal oxides is given in scheme-1²⁷.



Scheme. 1. synthetic scheme of Ag doped metal oxides

2.5 Antimicrobial activity of nanoparticles on MDR strains

The antimicrobial activity of Ag doped metal oxides samples against MDR strains (*E. coli*, *K. Pneumonia* and *S.aureus*) was evaluated by Agar well diffusion method on MHA by making a lawn of MDR strain with the aid of sterile cotton swabs. Wells of 6 mm diameter were punched carefully with the help of a cork borer and then the well was loaded with different concentrations of samples. The plates were incubated at 37°C for 24 h and antibacterial activity was determined by measuring the zone of inhibition.

2.6 Characterization

The structures of as prepared AgNPs and Ag doped metal oxides were studied by X – ray diffraction using X' Pert Pro X–ray diffractometer with Cu K α as source of radiation in a θ -2 θ configuration. Morphology and bonding of the above oxide was studied by SEM with X-ray analysis is efficient, inexpensive, and non-destructive to surface analysis. LEO 1530 field emission scanning electron microscope with EDX system from OXFORD is used. It is a high performance instrument designed for analytical applications featuring the GEMINI column technology. It is controlled by a 32-bit computer system using Microsoft Windows NT as an operating system. TEM images are carried out using Technai-20 Philips transmission electron microscope. The transmission electron microscope was operated at 190 KeV.

2.7 Technical details of Instruments

FT-IR: An electrical signal obtained from the IR through a narrow band electronic filter is passed through material and the complete spectrum could be measured by varying the filter frequency. A much more rapid approach is to use a digital computer to perform a Fourier transformation of the interferogram, thereby directly yielding the materials spectrum of the source, by instrument and any sample interposed in the optical path. The sample and KBr are mixed in the ratio 1:10 in a mortar and crushed to get a fine mixture. The KBr die and the plumpers were washed with water and acetone and dried before ~200 mg of the mixture was filled between the two plumpers and fixed in the die and then kept in the KBr pellet instrument to get a pellet. The hydraulic press was used to get the pellet which was then used for recording FT-IR Spectrum the range 500–4000 cm^{-1} .

XRD: X-ray diffraction tool is capable of investigating the crystalline structure of the materials, especially its symmetry. In addition, more than 90% solid materials are crystalline in nature and each crystalline has a unique X-ray diffraction pattern that can be used just like finger print in order to identify the materials. X-rays having wavelength λ bombarded the crystal materials with angle θ results scattered radiation, which can be determined by virtue of Bragg's law ($2d\sin\theta = n\lambda$). d-planes are unique for every material and manipulate different parameters like the geometry of incident rays and the orientation of the detector and materials. X' Pert Pro X-ray diffractometer with Cu $K\alpha$ as source is used in the present study and represents the obtained results in the form of indexed XRD pattern.

SEM and EDX: The scanning electron microscope produces images by scanning the sample with a high-energy beam of electrons. As the electrons interact with the sample, they produce secondary electrons from a filament and collimated into a beam in the electron source. The beam is then focused on the sample surface by a set of lenses in the electron column. Magnified images of an object are recorded by scanning its surface to create a high resolution image which shows the information about the object. EDX is used for the elemental identification and quantitative compositional information of the sample with the same electron bombardment. LEO 1530 field emission scanning electron microscope with EDX system from OXFORD is used in the present investigation.

TEM: It is an analytical technique used to visualize the smallest structures in matter. In this microscopy technique a **beam of electrons is transmitted through a specimen to form an image**. TEM can reveal stunning detail at the atomic scale by magnifying nanometre structures up to 50 million times. A heated tungsten filament in the electron gun generates a beam of electrons that is then focused on the specimen by the condenser to give the image. Technai-20 Philips transmission electron microscope was used for the high resolution sample images.

3. Results and discussion

3.1 X-ray diffraction analysis

Fig. 1 (a) shows the XRD pattern of a prepared AgNPs sample by combustion route using polymer fuel. The pattern shows the presence of intense Bragg's reflections due to the crystalline nature of the sample. The d-spacing estimations of the readied nano particles are coordinated well with standard 87-0720 JCPDS record of AgNPs. Unit cell parameters are recognized in above JCPDS. In the vast majority of the reflections (111), (200), (220), (311) are watched to demonstrate the arrangement of AgNPs. The unindexed crests in some specimens could be because of crystallization of biogenic states that happen on the surface of nanoparticles. All XRD design along these lines unmistakably demonstrates that the nanoparticles are framed by combustion lessening of nanoparticles.

Fig. 1(b-d) shows an indexed XRD pattern of as prepared Ag-MgO, Ag-NiO and Ag-ZnO NPs samples by combustion route respectively. These patterns show the presence of highly intense Bragg's reflections due to the crystalline nature of the sample. In addition to this, these patterns show the presence of Ag reflections along with the respective metal oxides peaks, which are identified in comparison with standard JCPDS files of respective metal oxides, which are given in **Table 2**. Presence of Ag reflection with metal oxides reflections confirms the formation of Ag doping with metal oxides. Referred JCPDS file and hkl values the samples are given in **Table 2**²⁸⁻³¹.

Table 2. JCPDS files and hkl values of the samples

Sl.No	Sample	Referred JCPDS files	hkl values
1	Ag	04-0783	(111) (200) (220) (311)
2	Ag-MgO	45-0946	(200) (220) (311)(222)
3	Ag-NiO	22-1189	(111) (200) (220) (222)
4	Ag-ZnO	87-0712	(101) (103) (102) (002)

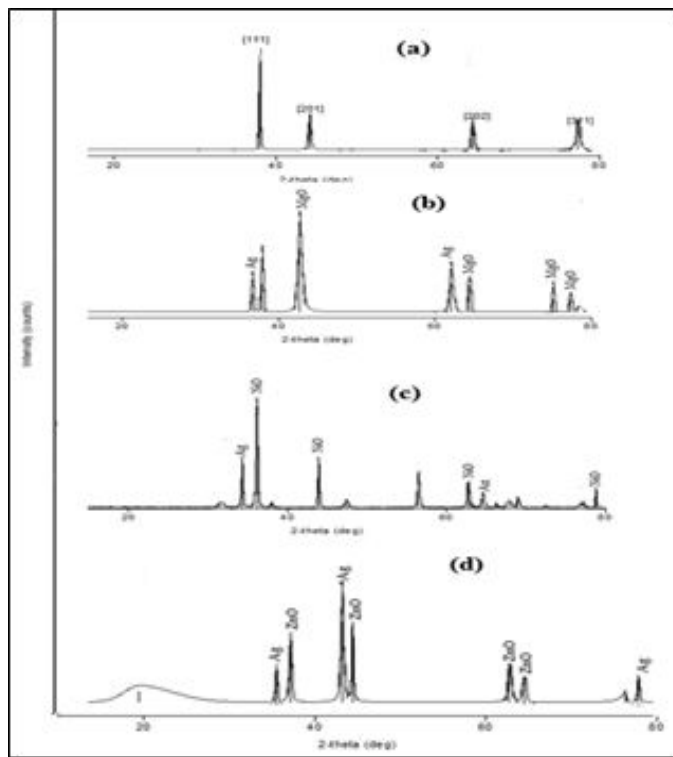


Fig. 1(a-d). XRD pattern of Ag, Ag-MgO, Ag-NiO and Ag-ZnO nanoparticles

3.2 Scanning Electron Microscopy analysis (SEM)

Field emission scanning electron microscope (FESEM) has been used to examine the morphology of the prepared nanoparticle samples. **Fig. 2** shows the SEM image of prepared AgNPs. The image shows fine formation of spherical shaped particles with dispersed structure. **Fig. 3(a-b)** shows SEM images of Ag-MgO nanoparticles at low and high resolution. The image shows irregular flowery type particles are grouped to form the crystalline nature. The same can be viewed clearly on high resolution. **Fig. 4(a-b)** SEM image of Ag-NiO nanocomposite at low and high resolution respectively. Crystalline morphology with irregular shaped particles is observed in the image. One can observe globular arrangement of particles mixing takes place. Irregular particles show the doped silver particles in the NiO can be viewed clearly in high resolution images. **Fig. 5(a-b)** SEM image of Ag-ZnO nanocomposite at low and high resolution respectively. Most of the spherical shaped particles define the crystalline nature of the prepared sample. A microcomposition of the silver nanoparticles in ZnO nanomaterials takes place. The increased particle compactness in the doped sample can be viewed clearly on a high resolution image.

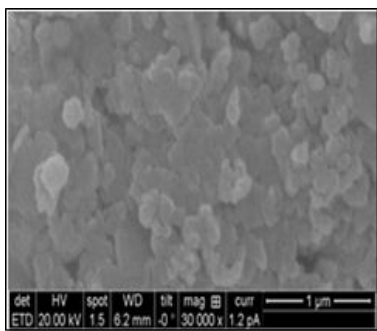


Fig. 2. SEM image of AgNPs

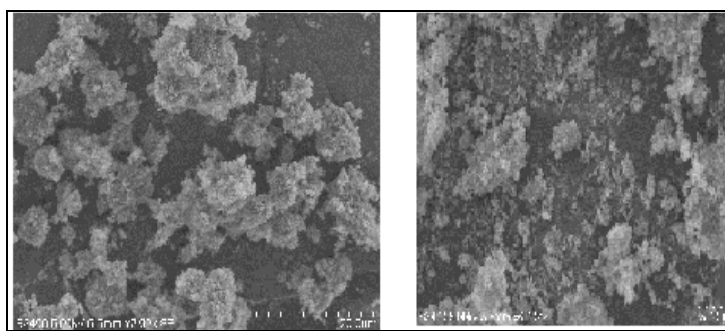


Fig. 3(a-b). SEM image of Ag-MgO at low and high resolution

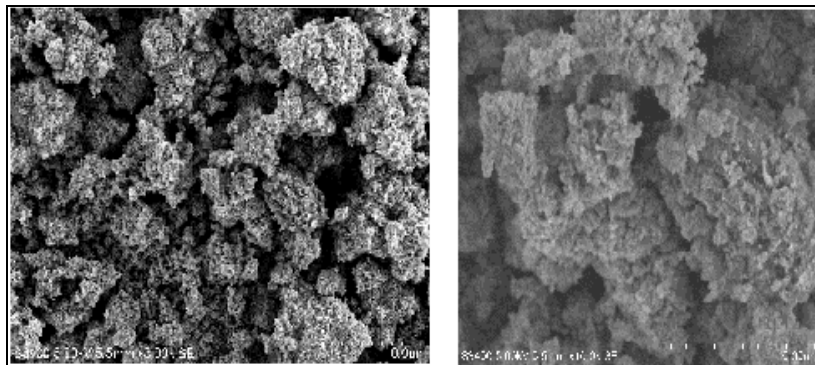


Fig. 4(a-b). SEM image of Ag-NiO at low and high resolution

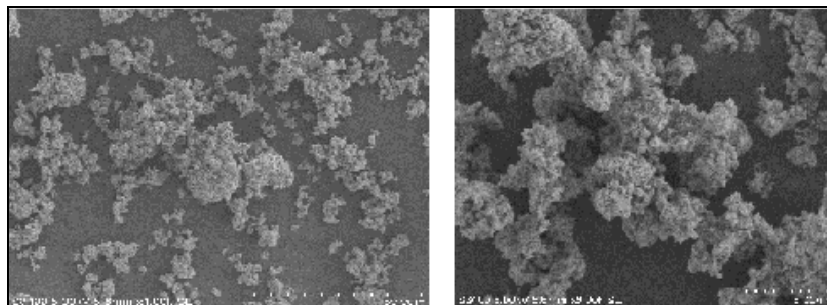


Fig. 5(a-b). SEM image of Ag-ZnO at low and high resolution

3.3 TEM analysis

Fig. 6 shows TEM image of representative Ag-MgO sample. This image shows most of the particles are spherical in nature and flowery in free assets. Some particles are agglomerated with each other and form a cloudy consideration. Almost all particles are in nanorange with imperfections in their surface centres. Doped Ag particles may vary the surface centre by occupying the same. Similar features may be observed for the Ag-NiO and Ag-ZnO samples.

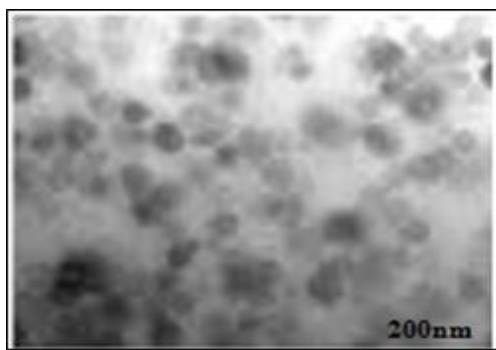


Fig. 6. TEM image of Ag-MgO sample

3.4 Energy Dispersive X-Rays (EDX) analysis

EDX report confirms a chemical composition or contaminants for the synthesized silver doped magnesium ferrite nanomaterials. **Fig. 7(a)** shows the EDX pattern of as prepared Ag NPs. The pattern showing Ag highest percentage signals at respective positions confirms the formation of Ag metal. Figure 7(b-c) shows the EDX pattern of Ag-MgO and Ag-ZnO samples respectively. The EDX spectrum gives the highest percentage signals of Mg and Zn along with silver for contaminants in nanoparticles. Presence of metals with silver metal in the pattern confirms the doping of Ag to the metal oxides.

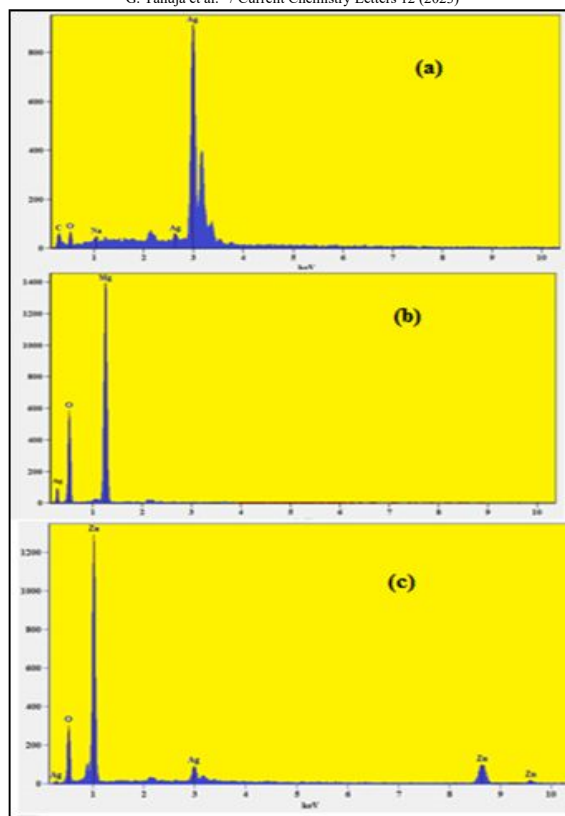


Fig. 7. EDX images of (a) Ag metal, (b) Ag-MgO and (c) Ag-ZnO nanoparticles

3.5 Infrared Study (FT-IR) analysis

Table 3 shows vibrational frequencies of as prepared Ag doped metal oxides. The metal-oxygen bonding and nature of the synthesized oxide sample was carried out by infrared study. Metal oxides generally give absorption bands below 1000 cm^{-1} arising from inter-atomic vibrations. The peak 3000 cm^{-1} corresponds to water of absorption. Vibrational frequency at 1500 cm^{-1} is due to the presence of carbon dioxide. Frequency at around 1200 cm^{-1} is due to some overtones. Peaks below 1000 cm^{-1} correspond to Metal-oxygen (M-O) vibrational modes of the samples conform to the formation of Ag doping magnesium ferrite.

Table 3. Vibrational frequencies of Ag metal and Ag-doped metal oxides

S.No	Vibrational frequencies (cm^{-1})		
	Ag-MgO	Ag-NiO	Ag-ZnO
1	3260	3230	3065
2	1540	1500	1450
3	1100	1050	1250
4	690	645	680
5	510	500	550
6	410	440	480
7	400	---	490
8	---	---	390

3.6 Antibacterial activity

The as-synthesized Ag-MgO and Ag-ZnO nanoparticles were tested for their antibacterial effect against the strain *Enterococcus faecalis* (A), *Klbesella pneumoniae*(B) *Staphylococcus aureus* (C) by agar well diffusion method. The results of the antibacterial activity of are illustrated in figure 8 and 9. The figures show that nanocomposite has good antibacterial activity and the bacteria cells have been killed at the respective concentration and results are given **Table 3** and **Table 4** respectively. In the present work chemically synthesized nanoparticles were examined for antibacterial activity against MDR isolates. Clinically isolated pathogens were inoculated in Luria-Bertani Broth and incubated at 37°C for 6 hrs, $100\ \mu\text{l}$ of each microorganism were inoculated on Muller Hinton Agar (MHA) plates: agar wells of 5mm diameter were prepared with the help of a sterilized steel cork borer. Different concentrations of the synthesized nanoparticles were used. Firstly, we have loaded samples with two different studies, i.e. variable in concentration of nanoparticles ($32\ \mu\text{l/ml}$) +constant

antibiotics and variable in concentration of antibiotics (16µl/ml) +constant nanoparticles. The concentration of nanoparticles is varied i.e. (20 µl, 32 µl, 40 µl) whereas the antibiotics were kept the same i.e. (10 µl). So the different concentration of nanoparticles and by keeping the antibiotics the same we have loaded the sample into the plates for every particular bacteria as mentioned above. The three well are made in which one of the well only nanoparticles are loaded and in the second well only the antibiotics samples are loaded and the last well the combination of the nanoparticles and the antibiotics are loaded which is then kept in the incubator for 24 hours at 37° for the better results. The obtained activity results of Ag-MgO are given table 4 and its zone of inhibition is given in figure 8. Secondly, the concentrations of the antibiotics are varied and the nanoparticles are kept the same. The concentration of the nanoparticles and the antibiotics are varied accordingly by keeping one or the other constant to check the zone of clearance for the particular bacteria. This shows the inhibition capacity of the nanoparticles or the antibiotics on the multi drug resistant bacteria. Similar feature is observed for Ag-ZnO and its activity results are given in table 5. The zone of inhibition of the activity experimentation of the sample is given in **Fig. 9**. These results indicate that; the prepared samples showed considerable antibacterial activity against represented bacteria.

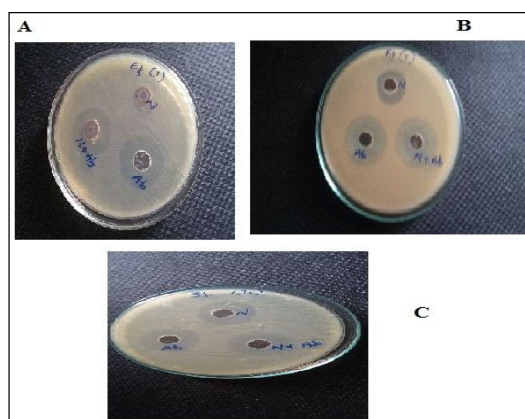


Fig. 8. Antibacterial activity of *Enterococcus faecalis* (A), *Klbesella pneumonia* (B) *Staphylococcus aureus* (C) for Ag-MgO

Table 4. Activity results of Ag-MgO sample

Pathogenic bacteria	Zone of inhibition (mm)		
	Antibacterial activity		Synergistic effect
	N	Ab	N+Ab
<i>Enterococcus faecalis</i>	12	15 (vacomicine)	18
<i>Klbesella pneumonia</i>	21	22 (ceftazidime)	26
<i>Staphylococcus aureus</i> MTCC	19	20 (mythacilin)	22

(N:Ag-MgO, Ab:antibio)

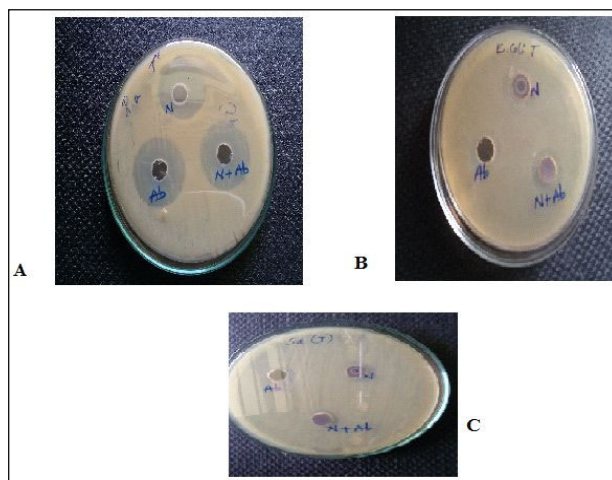


Fig. 9. Antibacterial activity of *Enterococcus faecalis* (A), *Klbesella pneumonia* (B) *Staphylococcus aureus* (C) for Ag-ZnO

Table 5. Activity results of Ag-ZnO sample

Pathogenic bacteria	Zone of inhibition (mm)		
	Antibacterial activity		Synergistic effect
	N	Ab	
E.coli	11	R (ceftriaxane)	15
Staphylococcus aureus MTCC	16	15 (mythacilin)	18
Pseudomonas aeruginosa	20	27 (ceftazadime)	23

(N:Ag- ZnO, Ab: antibio)

3. Conclusions

The bactericidal effect of silver doped metal oxide nanoparticles was studied against drug resistance microorganisms. The resistance and sensitivity of the MDR strains shows the zone of inhibition for the nanoparticles. As per the comparative study nanoparticle as antibacterial agent is considered as bactericidal if it kills bacteria or as bacteriostatic if it inhibits their growth. This concludes that the nanoparticles are more effective than those of antibiotics without any side effects.

Acknowledgement

Authors thank DST-FIST (SR/FST/CSI-003/2016) grant provided for instruments and infrastructure facilities at Department of studies in Chemistry, Vijayanagara Sri Krishnadevaraya University, Ballari. Thanks are due to Prof. A. Venkataraman, Professor, Department of Chemistry, Gulbarga University, Kalaburagi, Karnataka, India for useful discussion in spectral analysis.

References

- Lam.S. M., Quek, J. A. and Sin, J. C. (2018) Mechanistic investigation of visible light responsive Ag/ZnO micro/nanoflowers for enhanced photocatalytic performance and antibacterial activity. *Journal of Photochemistry and Photobiology A: Chemistry*, 353, 171–184; DOI; <https://doi.org/10.1016/j.jphotochem.2017.11.021>
- Avis T, Babu R Antony. (2019) Green synthesis of silver doped nano metal oxides of zinc & copper for antibacterial properties, adsorption, catalytic hydrogenation & photodegradation of aromatics, *J. Environ. Chem. Eng.* 7(1), 102840 ; DOI; <https://doi.org/10.1016/j.jece.2018.102840>
- Asmaa, M., Shafey., E. (2020) Green synthesis of metal and metal oxide nanoparticles from plant leaf extracts and their applications: A review. *Green Process. Synth.* 9(1), 304–339 ; DOI; <https://doi.org/10.1515/gps-2020-0031>
- Edwina. O., Uzunugbe, A., Paul K., Sixberth M., and Neerish R. (2020) Bio-inspired Synthesis of Acacia senegal Leaf Extract Functionalized Silver Nanoparticles and Its Antimicrobial Evaluation, *J. Nanomater.*, Article ID 6474913; DOI; <https://doi.org/10.1155/2020/6474913>
- Arunkumar Lagashetty, Sangappa K Ganiger, Preeti R. K. Shashidhar Reddy. (2020) Green Synthesis, Characterization and Antibacterial Study of Ag-Au Bimetallic Nanocomposite using Tea Powder Extract. *Biointerface Res. Appl. Chem.* 11(1), 8087–8095; DOI; <https://doi.org/10.33263/BRIAC111.80878095>
- Mangala S. Nagasundaria, Muthua K. Kaviyarasu K. Dunia A. AlFarraj Roua M. Alkufeidy. (2021) Current trends of Silver doped Zinc oxide nanowires photocatalytic degradation for energy and environmental application. *Surf. Interfaces*, 23, 100931 ;DOI; <https://doi.org/10.1016/j.surfin.2021.100931>
- Jicksy. J., Mithun S., Gurumurthy R., Thomas, M., Balachandran. (2021) Biosynthesized Ag Nanoparticles: a Promising Pathway for Bandgap Tailoring. *Biointerface Res. Appl. Chem.* 11(2), 8875 – 8883 ; DOI; <https://doi.org/10.33263/BRIAC112.88758883>
- Emilin R., Smitha. I., Chamarthy S., Sahithya. A., Samrot. V., Abirami S., Dhiva S., Daniel Alex Anand. (2021) Synthesis, Characterization, and Antibacterial Activity of Biosynthesized Gold Nanoparticles, *Biointerface Res. Appl. Chem.* 11(2) 9619 – 9628 ; DOI; <https://doi.org/10.33263/BRIAC112.96199628>
- Raji, P., Samrot, A.V., Keerthana., D. Karishma, S. (2019) Antibacterial Activity of Alkaloids, Flavonoids, Saponins and Tannins Mediated Green Synthesised Silver Nanoparticles Against Pseudomonas aeruginosa and Bacillus subtilis. *J Clust Sci.* 30, 881-895 ; DOI; <https://doi.org/10.1007/s10876-019-01547-2>
- Samrot, A.S.; Silky, V.I.C. Raji, P. SaiPriya, C. and Selvarani, J.A. (2019) Bioactivity Studies of Datura metel, Aegle marmelos, Annona recifulata and Saraca indica and their Green Synthesized Silver Nanoparticle. *J Pure Appl Microbiol* 13, 329-338 ; DOI; <https://dx.doi.org/10.22207/JPAM.13.1.36>
- Keijok, W.J. Pereira, R. H.A. Alvarez, L.A.C. (2019) Controlled biosynthesis of gold nanoparticles with Coffea arabica using factorial design. *Sci Rep* 9, 16019 ; DOI; <https://doi.org/10.1038/s41598-019-52496-9>
- Lee, K.X. Shameli, K.Yew, Y.P. Teow, S.Y. Jahangirian, H. Rafiee-Moghaddam, R. Webster, T.J.Recent. (2020) Developments in the Facile Bio-Synthesis of Gold Nanoparticles (AuNPs) and Their Biomedical Applications. *Int J Nanomedicine* 15, 275–300 ; DOI; <https://doi.org/10.2147/IJN.S233789>
- Khatua, A. Priyadarshini, E. Rajamani, P. Patel, A.; Kumar, J. Naik, A. Saravanan, M. Barabadi, H. Prasad, A. Paul, B. Meena, R. (2020) Photosynthesis, characterization and fungicidal potential of emerging gold nanoparticles

- using *Pongamia pinnata* leave extract: a novel approach in nanoparticle synthesis. *J Clust Sci* 31, 125-131; DOI; <https://doi.org/10.1007/s10876-019-01624-6>
14. Susanta Kumar Biswal., Manoranjan Behera., Ardhendu Sekhar Rout., Arpita Tripathy. (2021) Green Synthesis of Silver Nanoparticles Using Raw Fruit Extract of *Mimusops elengi* and their Antimicrobial Study, *Biointerface Res. Appl. Chem.*, 11(3), 10040 - 10051; DOI; <https://doi.org/10.33263/BRIAC113.1004010051>
 15. Arunkumar L., Manjunath K. P., Sangappa K. G. (2019) Green Synthesis, Characterization, and Thermal Study of Silver Nanoparticles by *Achras sapota*, *Psidium guajava*, and *Azadirachta indica* Plant Extracts, *Plasmonics*.14, 1219–1226;DOI; <https://doi.org/10.1007/s11468-019-00910-3>
 16. Buszewski, B. Railean-Plugaru, V. Pomastowski, P. Rafińska, K. Szultka-Mlynska, M. Golinska, P. Wypij, M. Laskowski, D. Dahm, H. (2018) Antimicrobial activity of biosilver nanoparticles produced by a novel *Streptacidiphilus durhamensis* strain. *J Microbiol Immunol Infect* 51, 45-54 ; DOI; <https://doi.org/10.1016/j.jmii.2016.03.002>
 17. Rajput, V. Minkina, T. Ahmed, B., Sushkova, S., Singh, R. Soldatov, M. Laratte, B. Fedorenko, A. Mandzhieva, S. Blicharska, E. Musarrat, J. Saquib, Q. Flieger, J. Gorovtsov, A. (2020) Interaction of Copper-Based Nanoparticles to Soil, Terrestrial, and Aquatic Systems: Critical Review of the State of the Science and Future Perspectives. *Rev Environ Contam & Toxicol* 252, 51-96; DOI; https://doi.org/10.1007/398_2019_34
 18. Ganiger, S.K. Murugendrappa, M.V. (2018) Lab Scale Study on Humidity Sensing and D.C. Conductivity of Polypyrrole/Strontium Arsenate ($\text{Sr}_3(\text{AsO}_4)_2$) Ceramic Composites. *POLYM SCI SER A+* 60, 395-404; DOI; <https://doi.org/10.1134/S1560090418030119>
 19. Lagashetty, A. Pattar, A. Ganiger.S.K. (2019) Synthesis, characterization and antibacterial study of Ag doped magnesium ferrite nanocomposite. *Heliyon* 5; DOI; <https://doi.org/10.1016/j.heliyon.2019.e01760>
 20. Lagashetty, A. Ganiger, S.K. Shashidhar. (2019) Synthesis, characterization and antibacterial study of Ag–Au Bi-metallic nanocomposite by bioreduction using piper beetle leaf extract. *Heliyon* 5; DOI; <https://doi.org/10.1016/j.heliyon>
 21. Lagashetty, A. Ganiger, S.K. Reddy, S. (2020) Microwave Derived Nano Sized Zirconium Vanadate as an Adsorbent for Heavy Metal Ions, *Lett. Appl. NanoBioScience* 9(3), 1420-1426; DOI; <https://doi.org/10.33263/LIANBS93.14201426>
 22. Annu, A. Ali., Shakeel A. (2019) Green Synthesis of Metal, Metal Oxide Nanoparticles, and Their Various Applications. *Handbook of Eco materials*, 2281-2325;DOI; https://doi.org/10.1007/978-3-319-68255-6_115
 23. Unuofin, J.O. Oladipo, A.O. Msagati, T.A.M. Lebelo, S.L. Meddows-Taylor, S. More, G.K. (2020) Novel silver-platinum bimetallic nanoalloy synthesized from *Vernonia mespilifolia* extract: Antioxidant, antimicrobial, and cytotoxic activities. *Arab. J. Chem.*, 2712; DOI; <https://doi.org/10.1016/j.arabjc.2020.06.019>
 24. Fierascu, I. Fierascu, I.C. Brazdis, R.I. Baroi, A.M. Fistos, T. Fierascu, R.C. (2020) Phytosynthesized Metallic Nanoparticles—between Nanomedicine and Toxicology. A Brief Review of 2019's Findings. *Materials* 13; DOI; <https://doi.org/10.3390/ma13030574>
 25. Saba, G. Faeze, F. Saeed, B. (2020) Phytochemical Synthesis of Silver Nanoparticles Using *Anthemis Nobilis* Extract and Its Antibacterial Activity. *Zeitschrift für Physikalische Chemie*, 234, 531-540; DOI; <https://doi.org/10.1515/zpch-2018-1288>
 26. Panchal, P. Paul, D.R.Sharma, A. Choudhary, P. Meena, P. Nehra, S.P. (2020) Biogenic mediated Ag/ZnO nanocomposites for photocatalytic and antibacterial activities towards disinfection of water. *J. Colloid Interface Sci.* 563, 370-380; DOI; <https://doi.org/10.1016/j.jcis.2019.12.079>
 27. Mickymaray, S. (2019) One-step Synthesis of Silver Nanoparticles Using Saudi Arabian Desert Seasonal Plant *Sisymbrium irio* and Antibacterial Activity Against Multidrug-Resistant Bacterial Strains. *Biomolecules*, 9, 662-669; DOI; <https://doi.org/10.3390/biom9110662>
 28. Chlebda D.K., Jędrzejczyk R.J., Jodłowski P.J. (2017) Surface structure of cobalt, palladium, and mixed oxide-based catalysts and their activity in methane combustion studied by means of micro-Raman spectroscopy, *Journal of Raman Spectroscopy*, 48(12), 1871-1880;DOI; <https://doi.org/10.1002/jrs.5261>
 29. Chlebda D.K., Stachurska P., Jędrzejczyk R.J., Kuterasiński Ł., Dziedzicka A., Górecka S., Chmielarz L., Łojewska J., Sitarz M., Jodłowski P. (2018) DeNO_x Abatement over Sonically Prepared Iron-Substituted Y, USY and MFI Zeolite Catalysts in Lean Exhaust Gas Conditions, *Nanomaterials (Basel)*, 3(1), 21 ;DOI; <https://doi.org/10.3390/nano8010021>
 30. Dereje Agonafer James Beck Kevin Cole W.J. Minkowycz Filippo de Monte Robert McMasters Keith Woodbur, (2018) Professor A. Haji-Sheikh on his 85th birthday. *Int. J. Heat Mass Transf.* 123, 1253–1254. <https://doi.org/10.1016/j.ijheatmasstransfer.2017.02.019>

